

previously proposed for other dusty rings (17, 20), where small grains released from the arc drift outward under the influence of nongravitational drag forces (such as plasma drag) while they are steadily eroded by collisions with ions, atoms, and smaller grains.

Consider that the visible arc represents dust released from the surfaces of larger bodies by collisions. Although the source bodies are trapped in the Mimas resonance, interactions with Saturn's magnetosphere allow dust to escape this region (17). The magnetospheric plasma corotates with the planet's magnetic field (period ~ 0.45 days) (21), so its mean motion is much faster than the dust grains' Keplerian orbital motion. Momentum transfer from the plasma therefore causes the dust to drift outward over time. For a particle of mass m located at semimajor axis a and with an orbital velocity v , a drag force F_D will cause a motion $da/dt = a/v(F_D/m)$. In general, F_D is proportional to the particle's surface area whereas m is proportional to its volume, so $da/dt \propto 1/s$, where s is the dust grain's linear size.

As the dust grains drift outward, they will be steadily eroded by collisions with plasma ions, energetic particles, and other small grains. So long as the collisions do not completely shatter the drifting grain (17), the mass loss rate will be proportional to the impactor flux times the grain's cross-sectional area, so $dm/dt \propto s^2$ and $ds/dt \propto s^0$. Thus, $ds/da \propto s$. Given that the G ring is narrow ($\delta a/a \sim 0.05$) and assuming that the drag forces and erosion rates do not vary significantly across this region, s should therefore decay exponentially with distance from the source region δa ; that is, $s = s_0 e^{-\delta a/3D}$, where s_0 is the initial particle

size, e is the base of natural logarithms, and $3D$ is a scale length determined by the orbital and magnetospheric environments.

The G ring's brightness and optical depth τ at a given δa are proportional to the integral of the particle cross section over the differential particle size distribution at that location [$\tau = \int \pi s^2 n(s, \delta a) ds$]. Assuming that the ring is in a steady state, continuity requires that the number flux of particles of a size s at a distance δa from the arc equal the flux of particles of size s_0 released from the arc, which requires that $n(s, \delta a) = n(s_0, 0)$ (see SOM). Hence, τ scales like s^3 and the optical depth also decreases exponentially with radial distance from the arc/source, but with a scale length of D instead of $3D$: $\tau = \tau_0 e^{-\delta a/D}$. This simple, generic model therefore produces a radial brightness profile with the same basic shape as that observed in the remote-sensing data. Furthermore, the shorter scale length in the optical depth means that although the brightness of the ring at 176,700 km is reduced by over an order of magnitude, individual particle sizes are reduced by only a factor of 2 or 3, so the grain detected by CDA could have been as small as about 200 μm across when it escaped the arc (that is, still small enough to be subject to non-gravitational accelerations).

References and Notes

1. M. R. Showalter, J. N. Cuzzi, *Icarus* **103**, 124 (1993).
2. R. Canup, L. W. Esposito, *Icarus* **126**, 28 (1997).
3. H. B. Throop, L. W. Esposito, *Icarus* **131**, 152 (1998).
4. J. J. Lissauer, R. G. French, *Icarus* **146**, 12 (2000).
5. I. dePater, S. C. Martin, M. R. Showalter, *Icarus* **172**, 446 (2004).
6. C. C. Porco *et al.*, *Space Sci. Rev.* **115**, 363 (2004).

7. R. A. Jacobson *et al.*, *Astron. J.* **132**, 2520 (2006).
8. Mimas' 7:6 inner Lindblad resonance also lies nearby at $445.411^\circ/\text{day}$ ($a = 167,511$ km).
9. P. Goldreich, S. Tremaine, N. Borderies, *Astron. J.* **92**, 490 (1986).
10. C. C. Porco, *Science* **253**, 995 (1991).
11. F. Namouni, C. C. Porco, *Nature* **417**, 45 (2002).
12. J. A. van Allen, *J. Geophys. Res.* **88**, 6911 (1983).
13. S. M. Krimigis *et al.*, *Space Sci. Rev.* **114**, 233 (2004).
14. G. H. Jones *et al.*, *Science* **311**, 1412 (2006).
15. E. Roussos *et al.*, *Icarus*, in press.
16. J. N. Cuzzi, J. A. Burns, *Icarus* **74**, 284 (1988).
17. J. A. Burns, D. P. Hamilton, M. R. Showalter, in *Interplanetary Dust*, E. Grün, B. Gustafson, S. Dermott, H. Fechtig, Eds. (Springer, New York, 2001), pp. 641–725.
18. Slight deviations from an exponential profile occur around 168,200 and 169,800 km. The latter feature shows longitudinal structure and is probably associated with the Mimas 8:7 inner Lindblad resonance.
19. R. Srama *et al.*, *Space Sci. Rev.* **114**, 465 (2004).
20. J. A. Burns, M. R. Showalter, G. E. Morfill, in *Planetary Rings*, R. Greenberg, A. Brahic, Eds. (Univ. of Arizona Press, Tucson, AZ, 1984), pp. 200–272.
21. D. Gurnett *et al.*, *Science* **316**, 442 (2007).
22. We thank the staff at the Space Science Institute, Jet Propulsion Laboratory, and Cornell University for planning and delivering the imaging data, and M. Kusterer of the Johns Hopkins University Applied Physics Laboratory (JHUAPL) for LEMMS data reduction. We also acknowledge the support of the Cassini Project and NASA's Planetary Geology & Geophysics program. MIMI/LEMMS was in part financed by the German Bundesministerium für Bildung und Forschung through the German Aerospace Center (DLR) under contract 50 OH 0103 and by the Max Planck Gesellschaft. The work at JHUAPL was supported by NASA under contract NAS5-97271 with the Johns Hopkins University. G.H.J. was partially supported by the Science and Technology Facilities Council, UK.

18 April 2007; accepted 14 June 2007
10.1126/science.1143964

The FERONIA Receptor-like Kinase Mediates Male-Female Interactions During Pollen Tube Reception

Juan-Miguel Escobar-Restrepo,¹ Norbert Huck,¹ Sharon Kessler,¹ Valeria Gagliardini,¹ Jacqueline Gheyselinck,¹ Wei-Cai Yang,² Ueli Grossniklaus^{1*}

In flowering plants, signaling between the male pollen tube and the synergid cells of the female gametophyte is required for fertilization. In the *Arabidopsis thaliana* mutant *feronia* (*fer*), fertilization is impaired; the pollen tube fails to arrest and thus continues to grow inside the female gametophyte. *FER* encodes a synergid-expressed, plasma membrane-localized receptor-like kinase. We found that the FER protein accumulates asymmetrically in the synergid membrane at the filiform apparatus. Interspecific crosses using pollen from *Arabidopsis lyrata* and *Cardamine flexuosa* on *A. thaliana* stigmas resulted in a *fer*-like phenotype that correlates with sequence divergence in the extracellular domain of FER. Our findings show that the female control of pollen tube reception is based on a FER-dependent signaling pathway, which may play a role in reproductive isolation barriers.

In contrast to animals, where the products of meiosis differentiate directly into gametes, the meiotic products of higher plants undergo further mitotic divisions to form multicellular haploid structures called gameto-

phytes, which in turn produce the gametes. To accomplish fertilization, the gametophytes communicate with and recognize each other. In angiosperms, the male gametophyte (pollen) germinates on the stigma and the growing pollen

tube delivers the two nonmotile sperm cells to the female gametophyte (embryo sac). Proper delivery depends on signals from the female gametophyte (1, 2). These chemotactic signals guide the pollen tube into the micropylar opening of the ovule, the reproductive structure that harbors the female gametophyte. In the majority of flowering plants, including *Arabidopsis thaliana* (Brassicaceae), the female gametophyte consists of seven cells: the egg cell, the two synergids (which lie just inside the micropylar opening of the ovule), the central cell, and the three antipodals (3) (Fig. 1A). In *Torenia fournieri* (Scrophulariaceae), the two synergids are necessary for pollen tube guidance (4). In most species, one of the synergids degenerates prior to or coincident with the pollen tube approaching the micropyle (5). The pollen tube grows into the degenerating synergid through the filiform apparatus, a structure formed by invaginations of the cell wall of

¹Institute of Plant Biology and Zürich-Basel Plant Science Center, University of Zürich, Zollikerstrasse 107, CH-8008 Zürich, Switzerland. ²Key Laboratory of Molecular and Developmental Biology, Institute of Genetics and Developmental Biology, Chinese Academy of Sciences, Beijing 100101, China.

*To whom correspondence should be addressed. E-mail: grossnik@botinst.uzh.ch

both synergids (6). Pollen tube reception in the ovule involves the arrest of pollen tube growth (Fig. 1B), the rupture of the pollen tube, and the release of the sperm cells, which are subsequently targeted to the egg and central cells for fertilization (7). Once the pollen tube has ruptured, attraction of further pollen tubes ceases; thus, only a single pollen tube will normally enter each micropyle.

Recent work in *A. thaliana* has shown that pollen tube reception is controlled by female gametophytic factors (8, 9). In heterozygous *feronia* (*fer*) and *sirène* (*sir*) mutants, all female gametophytes develop normally but half of the ovules remain unfertilized. In these ovules, the pollen tube continues to grow inside the female gametophyte, fails to arrest its growth, and does not rupture to release the sperm cells (Fig. 1C). Pollen from these mutants, however, can fertilize wild-type ovules, indicating that pollen tube growth and sperm delivery are unaffected (8, 9). Detailed cytological and ultrastructural analyses have shown that the synergids are normally specified and differentiated (8), which suggests that these mutants identify components of an active signaling process in which female gametophytic factors control pollen tube behavior and hence fertilization. Only a small number of factors involved in pollen germination, pollen tube growth, and guidance are known at the molecular level (10–15). The molecular events

underlying the female control of pollen tube reception are unknown. Here, we show that *FER* encodes a kinase-active receptor-like kinase, which is localized to the plasma membrane and, in particular, is asymmetrically localized to the filiform apparatus of the synergid cells. Interspecific crosses indicate that the interaction of the *FER* receptor-like kinase with a putative ligand on the pollen tube may be involved in reproductive isolation barriers.

To gain insight into the molecular basis of the signaling event underlying pollen tube reception, we molecularly cloned *FER* with the use of positional methods (16). We mapped the mutation to At3g51550, which in the *fer* mutant contains a 4-base pair (bp) insertion corresponding to the footprint left after excision of a *Ds* transposon (Fig. 1D). Because *sir* shows the same phenotype, we sequenced the coding region of At3g51550 in the mutant and found a single base pair deletion (Fig. 1E). Both mutations lead to frameshifts that result in premature stop codons; therefore, *FER* and *SIR* are allelic.

A genomic fragment carrying At3g51550 plus 2.6 kb and 1.2 kb of upstream and downstream sequences, respectively, complements the *fer* phenotype (table S1), demonstrating that At3g51550 corresponds to the *FER* gene (fig. S1, A and B). The *FER* open reading frame contains a single 175-bp intron in the 5' untranslated region and produces a transcript of 2682 bp, which encodes

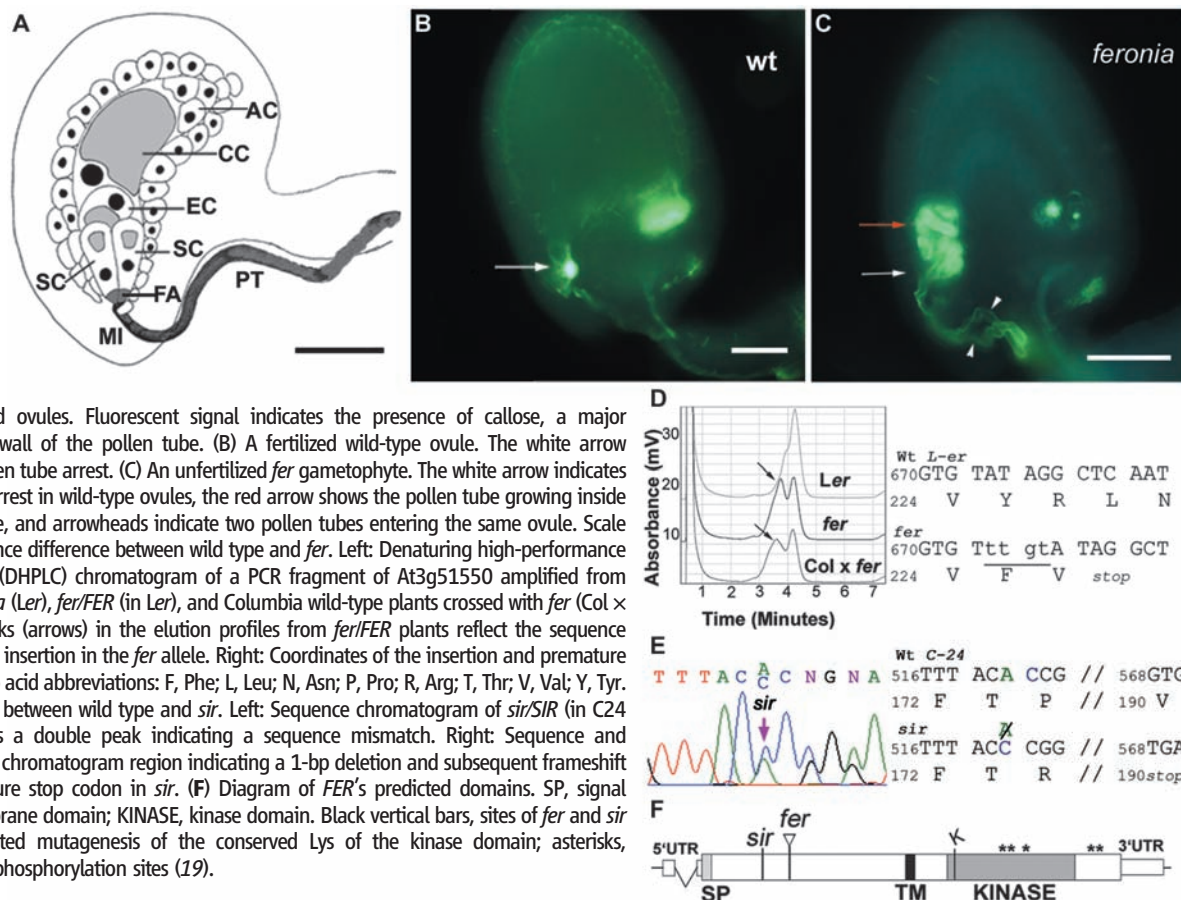
a putative receptor-like serine-threonine kinase (RLK) (Fig. 1F).

FER, which is a unique gene in *A. thaliana*, belongs to the CrRLK1L-1 subfamily of kinases, no members of which have a known function (Fig. 2A) (17). Plant RLKs belong to a monophyletic gene family with more than 600 members (18). RLKs are transmembrane proteins that receive signals through an extracellular domain and subsequently activate signaling cascades via their intracellular kinase domain, a molecular function consistent with the role of *FER* in a signaling process.

To determine the activity of the predicted intracellular kinase domain, we tested whether *FER* autophosphorylates in an in vitro kinase assay. The predicted intracellular domain (*FER*wt) and a kinase-inactive version (*FER*KR) were fused to glutathione *S*-transferase (*GST*). *GST* and *GST-FER*KR exhibited no kinase activity, whereas *GST-FER*wt was autophosphorylated (Fig. 2B). In addition, experimentally verified phosphorylation sites were present in the *FER* kinase domain (19) (Fig. 1F). Taken together, these findings show that *FER* encodes a kinase-active RLK involved in a novel signaling pathway that plays a critical role in the last stages of the communication between female and male gametophytes required for fertilization.

To evaluate whether the expression of *FER* is consistent with its proposed role in pollen tube

Fig. 1. Pollen tube reception is mediated by the FERONIA RLK. (A) Diagram of a mature female gametophyte. Abbreviations: AC, antipodal cells; CC, central cell; EC, egg cell; SC, synergid cells; FA, filiform apparatus; MI, micropyle; PT, pollen tube. Scale bar, 30 μ m. (B and C) Epifluorescence micrographs of Aniline Blue-stained ovules. Fluorescent signal indicates the presence of callose, a major component of the cell wall of the pollen tube. (B) A fertilized wild-type ovule. The white arrow indicates the site of pollen tube arrest. (C) An unfertilized *fer* gametophyte. The white arrow indicates the site of pollen tube arrest in wild-type ovules, the red arrow shows the pollen tube growing inside the female gametophyte, and arrowheads indicate two pollen tubes entering the same ovule. Scale bars, 30 μ m. (D) Sequence difference between wild type and *fer*. Left: Denaturing high-performance liquid chromatography (DHPLC) chromatogram of a PCR fragment of At3g51550 amplified from DNA of Landsberg *erecta* (*Ler*), *fer*/*FER* (in *Ler*), and Columbia wild-type plants crossed with *fer* (*Col* \times *fer*). The additional peaks (arrows) in the elution profiles from *fer*/*FER* plants reflect the sequence difference due to a 4-bp insertion in the *fer* allele. Right: Coordinates of the insertion and premature stop codon in *fer*. Amino acid abbreviations: F, Phe; L, Leu; N, Asn; P, Pro; R, Arg; T, Thr; V, Val; Y, Tyr. (E) Sequence difference between wild type and *sir*. Left: Sequence chromatogram of *sir*/*SIR* (in C24 accession); arrow shows a double peak indicating a sequence mismatch. Right: Sequence and coordinates of the same chromatogram region indicating a 1-bp deletion and subsequent frameshift that leads to a premature stop codon in *sir*. (F) Diagram of *FER*'s predicted domains. SP, signal peptide; TM, transmembrane domain; KINASE, kinase domain. Black vertical bars, sites of *fer* and *sir* mutations; K, site-directed mutagenesis of the conserved Lys of the kinase domain; asterisks, experimentally located phosphorylation sites (19).



reception, we examined the temporal and spatial expression pattern of *FER*. Quantitative real-time reverse transcription polymerase chain reaction (RT-PCR) revealed *FER* mRNA throughout the mature plant—specifically in leaves, buds, flowers, and siliques—but it was not detected in mature pollen (Fig. 2C). By *in situ* hybridization, *FER* transcripts were detected in floral apices, young ovule primordia, and young anthers with immature pollen (Fig. 3, A to C). In older anthers harboring mature pollen, *FER* transcript was not detected (Fig. 3D), consistent with the quantitative real-time RT-PCR experiments and the female-specific role of *FER* in fertilization. In emasculated flowers, a very weak *FER* signal was detected throughout mature unfertilized ovules, and a stronger signal could be detected in the synergid cells (Fig. 3E). After fertilization, *FER* transcripts were detected in globular embryos (Fig. 3G), consistent with the finding that in rare cases where fertilization of *fer* gametophytes is achieved, the resulting homozygous embryos abort (8). In our complementation experiments, both the defect in pollen tube reception and embryo lethality were rescued by a wild-type *FER* transgene, demonstrating that *FER* is also required after fertilization (table S1). A genomic fragment containing the putative *FER* promoter (1.3 kb upstream of the start codon) was fused to the bacterial *uidA* gene encoding β -glucuronidase (*GUS*) to confirm the weak expression of *FER* observed in

mature female gametophytes. Using a chromogenic substrate for *GUS*, we found that the *FER* promoter is highly active in the synergid cells (Fig. 3, I and J). Thus, the spatiotemporal expression pattern of *FER* is consistent with a function in pollen tube reception.

To investigate the subcellular localization of *FER*, we bombarded onion epidermal cells with a *FER-GFP* construct driven by the *FER* promoter (*pFER::FER-GFP*). The *FER-GFP* (green fluorescent protein) fusion protein was localized to the plasma membrane (Fig. 4, A and B), in contrast to *GFP* driven by the constitutive 35S promoter (*35S::GFP*), which is detected throughout the cell (Fig. 4, C and E). The *pFER::FER-GFP* construct was also stably transformed into *A. thaliana* and fully complemented the *fer* mutation (table S1), and the fusion protein was localized at the plasma membrane in leaf epidermal cells (Fig. 4D). Unfertilized ovules accumulated high levels of *GFP* signal in the lower part of the synergids (Fig. 4F) where the filiform apparatus is located. Weaker *GFP* fluorescence was detected in the membranes of the synergid cells and in the surrounding maternal sporophytic cells, as well as faintly in the egg cell (Fig. 4G). Because the filiform apparatus is a structure rich in plasma membrane, we tested whether the asymmetric distribution of *FER* might simply be due to an enrichment of plasma membrane in the area. Therefore, we compared

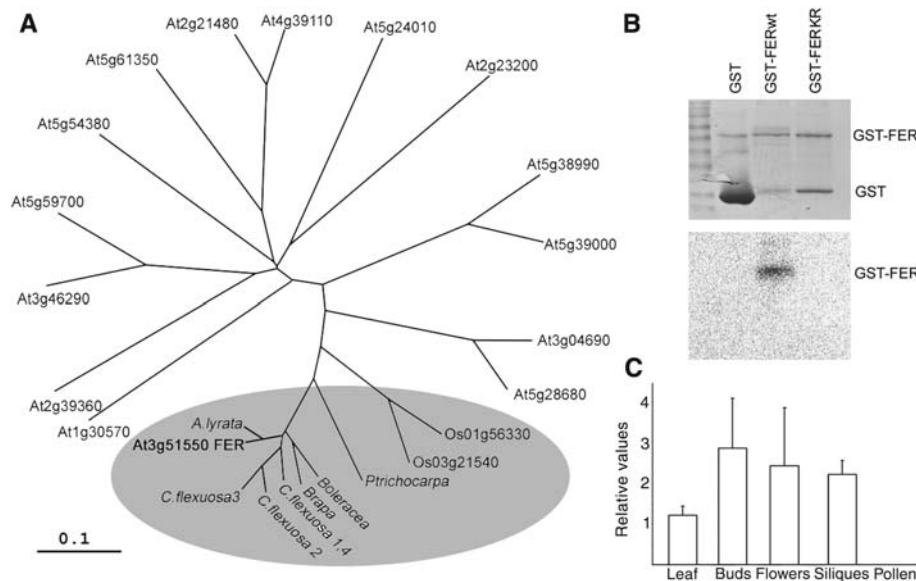


Fig. 2. *FERONIA*, a plant-specific, widely expressed RLK, phosphorylates itself. (A) Unrooted tree showing *FER* and homologs from different species. The *FER* homologs, whose clade is supported by a 100% bootstrap value, are in the shaded area. The other plant species together with *A. thaliana* in this clade are *A. lyrata*, *B. oleracea*, *B. rapa*, and *C. flexuosa* homologs 1, 2, 3, and 4 (Brassicaceae), *Oryza sativa* (Os., Poaceae), and *Populus trichocarpa* (Salicaceae). The rest of the tree contains the *A. thaliana* members of the CrRLK1L-1 subfamily of kinases. The branch length scale bar represents 0.1 substitutions per site. (B) *FER* autophosphorylates during *in vitro* kinase assays. Top: Coomassie-stained gel of proteins used in the kinase assays. Bottom: Phosphoimager scan of gel in top panel. GST and GST-*FER*KR (*FER* Lys⁵⁶³ → Arg in *Ler*, *FER* Lys⁵⁶⁵ → Arg in Col-0) have no kinase activity, whereas GST-*FER*wt is autophosphorylated. (C) Quantification of *FER* transcripts in leaves, closed flower buds, open flowers, and siliques (collected 1 to 4 days after hand pollination) and mature pollen grains. Transcript levels were normalized to 18S ribosomal RNA; means and SEs of three independent experiments are shown.

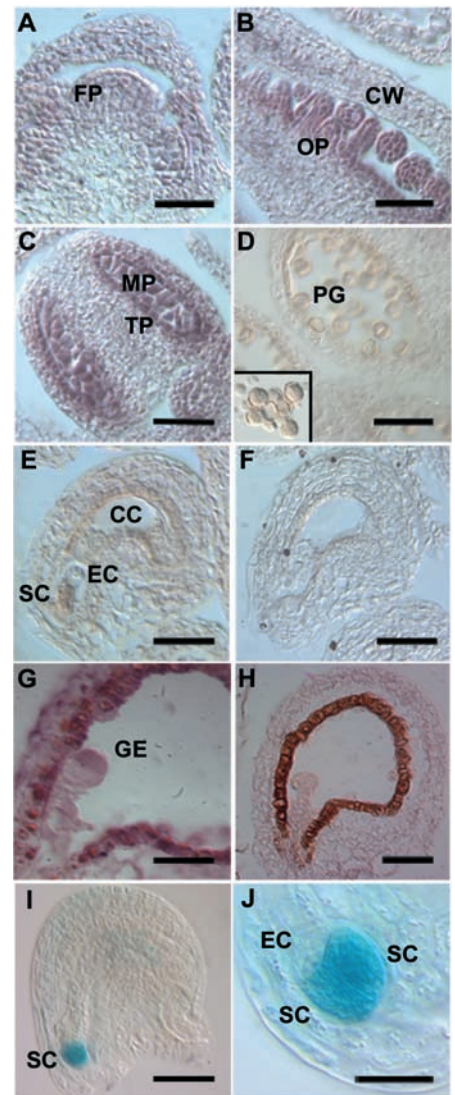


Fig. 3. *FERONIA* is expressed in developing primordia and synergid cells. (A to H) *In situ* hybridization with an antisense *FER* probe [(A) to (E), (G)] or with a sense probe [(F) and (H)]. *FER* mRNA is present in the floral apex (A) and in ovule primordia (B). *FER* mRNA is expressed in anthers and microspores during early pollen development (C), but the transcript levels in mature pollen (D) are below the limit of detection (inset shows the sense control). (E) *FER* transcript can be detected in the synergid cells of the female gametophyte. (F) Sense control in the female gametophyte. (G) After fertilization, *FER* mRNA was detected in globular embryos. (H) Sense control in a fertilized ovule with a globular embryo. (I and J) Analysis of the *FER* upstream transcriptional regulatory region. (I) *pFER::GUS* is active in both synergid cells. (J) Higher magnification of the synergids from another ovule. Scale bars, 100 μ m (A), 30 μ m [(B), (E), (F), (I), (J)], 15 μ m (C), 70 μ m (D), and 50 μ m [(G) and (H)]. Abbreviations: FP, floral apex; OP, ovule primordia; CW, carpal wall; MP, microspore cells; TP, tapetum cells; PG, pollen grain; CC, central cell; EC, egg cell; SC, synergid cell; GE, globular-stage embryo.

the distribution of FER to that of another GFP fusion construct that has a plasma membrane localization motif and is expressed in the female gametophyte (*pAtD123::EGFP-AtROP6C*). Under the same conditions, FER-GFP levels were much higher in the filiform apparatus than in the rest of the synergids' cell membranes when compared to EGFP-AtROP6C (Fig. 4H). This finding suggests that FER is polarly transported to the filiform apparatus. Taken together, the data are consistent with a model in which FER, localized in the filiform apparatus, binds a putative ligand on the approaching male gametophyte, which then triggers the molecular events involved in pollen tube reception.

Because a signal transduction cascade initiated by the interaction of the FER RLK with a putative pollen ligand seems necessary for fertilization, it is possible that changes in the components of this interaction could act as reproductive isolation barriers. To some extent, the interaction between the pollen tube and the synergid is similar to sperm-egg interactions in animals (20), but it occurs at the level of gametophytes rather than gametes. For example, divergence in the protein sequence of the putative ligand-binding extracellular domain of FER or changes in the pollen ligand could prevent interspecific fertilization events. Interestingly, in interspecific crosses of *Rhododendron* species, pollen tube growth does not arrest. This results in pollen tube overgrowth in the female gametophyte, similar to the phenotype observed in *fer* (21, 22). If our model is correct, an interspecific

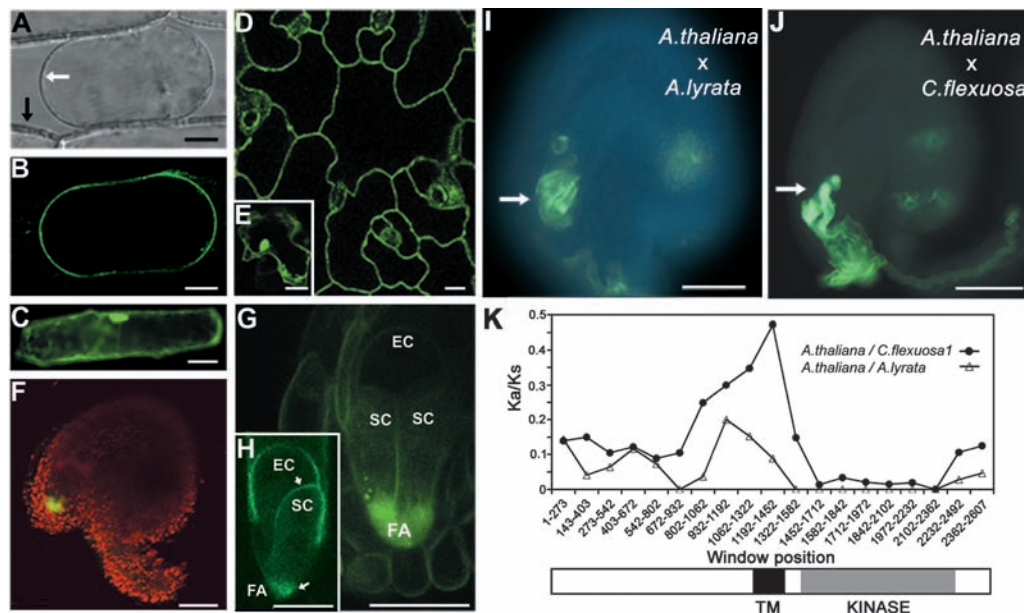
cross where wild-type *A. thaliana* is pollinated by a related Brassicaceae species with a sufficiently divergent ligand might also produce a *fer*-like phenotype. Therefore, we performed interspecific crosses between *A. thaliana* and different Brassicaceae species. In most crosses, the pollen germinated but failed to grow toward the ovules, as reported previously (23–26). In crosses with the close relative *Arabidopsis lyrata*, pollen tubes were correctly targeted to the ovule but only 43.9% of the embryo sacs received pollen tubes and were fertilized; 5.2% of the ovules were fertilized with more than one pollen tube in the same micropyle, showing pollen tube overgrowth inside the female gametophyte (fig. S1C); and 50.9% of the ovules had pollen tubes that continued to grow inside the female gametophyte, as was observed in *fer* mutants (Fig. 4I) ($n = 813$ ovules). In crosses with a more distant relative, *Cardamine flexuosa*, only 7.7% of *A. thaliana* ovules attracted pollen tubes; of these, 1.6% had pollen tubes that entered the micropyle and stopped as previously reported (27), 0.8% had pollen tubes coiling outside the micropyle, and in 5.3% of the ovules the pollen tubes entered the micropyles but reception failed, resulting in a *fer*-like phenotype ($n = 363$ ovules) (Fig. 4J). In summary, around 50% and 70% of the *A. lyrata* and *C. flexuosa* pollen tubes that entered a wild-type *A. thaliana* embryo sac, respectively, displayed a *fer*-like phenotype.

Given the involvement of the FER signal transduction cascade in the interaction between the pollen tube and the receptive synergid, it is

likely that FER plays a role in the failed pollen tube reception in these interspecific crosses. In the *A. thaliana* × *A. lyrata* crosses, about half of the pollen tube reception events were normal, demonstrating the capacity of the *A. lyrata* pollen tube for a normal reception response. However, in the same cross, *fer*-like phenotypes were observed. This suggests two possible reasons for failed receptions: (i) They are caused by a divergent ligand that is inefficiently recognized by the receptor domain of the *A. thaliana* FER RLK, or (ii) they result from the presence of two polymorphic forms of the putative ligand, one that is and one that is not recognized by the *A. thaliana* FER RLK. In the case of *C. flexuosa*, the ligand or ligands are predicted to have diverged to a degree that they cannot be recognized by the *A. thaliana* FER RLK, thereby causing the *fer*-like phenotype in *A. thaliana* ovules. We expect that a divergence in the sequence of the putative ligand would also be reflected in sequence divergence in FER's extracellular domain, which is proposed to interact with this ligand.

To test this hypothesis, we isolated FER homologs in these species and calculated the ratio between the number of nonsynonymous substitutions per nonsynonymous site (K_a) and the number of synonymous substitutions per synonymous site (K_s) (28) as an indication of their divergence in pairwise comparisons between *A. thaliana* and *A. lyrata* (one FER homolog) or *C. flexuosa* (four FER homologs) (Fig. 4K and fig. S1D). In all comparisons, higher K_a/K_s values occurred in the putative

Fig. 4. FERONIA is a cell membrane–localized RLK targeted to the filiform apparatus, and sequence divergence in its extracellular domain correlates with *feronia*-like phenotypes in interspecific crosses. (A) Transmission image of a plasmolyzed onion epidermal cell transiently expressing FER-GFP under FER promoter (*pFER::FER-GFP*). Black arrow points to cell wall; white arrow points to cell membrane. (B) Confocal laser scanning microscopy (CLSM) single optical section of (A) with FER-GFP localized at the periphery of the cell membrane. (C) Epifluorescence micrograph of an onion cell transiently expressing (*35S::GFP*). (D) CLSM single optical section of leaf epidermis of an *A. thaliana* plant stably transformed with *pFER::FER-GFP*. (E) *A. thaliana* leaf epidermal cell transiently expressing (*35S::GFP*). (F) Ovule from the same plant as in (D) under CLSM; GFP signal in green, chlorophyll autofluorescence in red. (G) Maximum projection of several sections of the micropyle area of ovule in (F) showing FER-GFP accumulation in the filiform apparatus of the synergids. (H) Maximum projection of several sections of *pAtD123::EGFP-AtROP6C* female gametophyte. Upper arrow indicates upper part of synergids; lower arrow indicates region of filiform apparatus. (I) Gametophyte of a wild-type *A. thaliana* plant pollinated with pollen from *A. lyrata*, showing pollen tube overgrowth (white arrow). (J) Gametophyte of a wild-type *A. thaliana* plant



pollinated with pollen from *C. flexuosa*, showing pollen tube overgrowth (white arrow). (K) K_a/K_s ratios calculated using a sliding window analysis with windows of 86 codons and a step size of 43 codons of the coding region of FER (excluding the signal peptide) in *A. thaliana*, *A. lyrata*, and *C. flexuosa* homolog 1. The least divergent homolog of *C. flexuosa* is shown. Scale bars, 30 μm [(A), (B), (F), (I), (J)], 60 μm (C), 10 μm [(D) and (E)], 20 μm [(G) and (H)]. SC, synergid cell; FA, filiform apparatus; EC, egg cell.

ligand-binding extracellular region, which indicates that this domain shows the greatest degree of amino acid diversification and evolves faster than the highly conserved intracellular kinase domain (29). The high sequence divergence in the extracellular domain of FER may contribute to reproductive isolation between two species, as has been proposed for other genes involved in recognition at fertilization (30).

Our data suggest that FER acts in the filiform apparatus to control the behavior of the pollen tube to achieve fertilization. We propose that the interaction between the putative male ligand and the extracellular domain of the FER RLK triggers a signal transduction cascade inside the synergid cell. A subsequent signal then feeds back from the synergid to the pollen tube, causing growth arrest and the release of the sperm cells. Conceptually, this process is similar to the signaling events occurring during the self-incompatibility reaction in *Brassica* spp. (31). In an incompatible pollination, a pollen ligand interacts with a stigma-expressed RLK, inducing a signaling cascade in female papillar cells, which then signal back to the pollen and inhibit its germination. Further studies of the FER signaling pathway will help to uncover the molecular mechanism of fertilization and reproductive isolation in plants. Furthermore, the manipulation of the FER pathway might allow the generation of hybrids between otherwise incompatible species.

References and Notes

- M. Hülkamp, K. Schneitz, R. E. Pruitt, *Plant Cell* **7**, 57 (1995).
- S. M. Ray, S. S. Park, A. Ray, *Development* **124**, 2489 (1997).
- U. Grossniklaus, K. Schneitz, *Semin. Cell Dev. Biol.* **9**, 227 (1998).
- T. Higashiyama *et al.*, *Science* **293**, 1480 (2001).
- R. N. Kapil, A. K. Bhatnagar, *Phytomorphology* **25**, 334 (1975).
- B. Q. Huang, S. D. Russell, *Int. Rev. Cytol.* **140**, 233 (1992).
- S. D. Russell, *Int. Rev. Cytol.* **140**, 357 (1992).
- N. Huck, J. M. Moore, M. Federer, U. Grossniklaus, *Development* **130**, 2149 (2003).
- N. Rotman *et al.*, *Curr. Biol.* **13**, 432 (2003).
- C. R. Schopfer, M. E. Nasrallah, J. B. Nasrallah, *Science* **286**, 1697 (1999).
- M. Mishima *et al.*, *J. Biol. Chem.* **278**, 36389 (2003).
- S. Kim *et al.*, *Proc. Natl. Acad. Sci. U.S.A.* **100**, 16125 (2003).
- M. L. Márton, S. Cordts, J. Broadvest, T. Dresselhaus, *Science* **307**, 573 (2005).
- W. Tang, D. Kelley, I. Ezcurra, R. Cotter, S. McCormick, *Plant J.* **39**, 343 (2004).
- K. von Besser, A. C. Frank, M. A. Johnson, D. Preuss, *Development* **133**, 4761 (2006).
- See supporting material on Science Online.
- S. H. Shiu, A. B. Bleeker, *Plant Physiol.* **132**, 530 (2003).
- S. H. Shiu, A. B. Bleeker, *Proc. Natl. Acad. Sci. U.S.A.* **98**, 10763 (2001).
- T. S. Nuhse, A. Stensballe, O. N. Jensen, S. C. Peck, *Plant Cell* **16**, 2394 (2004).
- P. Primakoff, D. G. Myles, *Science* **296**, 2183 (2002).
- V. Kaul, J. L. Rouse, E. G. Williams, *Can. J. Bot.* **64**, 282 (1986).
- E. G. Williams, V. Kaul, J. L. Rouse, B. F. Palsler, *Aust. J. Bot.* **34**, 413 (1986).
- S. J. Hiscock, H. G. Dickinson, *Theor. Appl. Genet.* **86**, 744 (1993).
- M. K. Kandasamy, J. B. Nasrallah, M. E. Nasrallah, *Development* **120**, 3405 (1994).
- M. Hülkamp, S. D. Kopczak, T. F. Horejsi, B. K. Kihl, R. E. Pruitt, *Plant J.* **8**, 703 (1995).
- K. K. Shimizu, K. Okada, *Development* **127**, 4511 (2000).
- K. K. Shimizu, *Popul. Ecol.* **44**, 221 (2002).
- M. Nei, T. Gojobori, *Mol. Biol. Evol.* **3**, 418 (1986).
- S. H. Shiu *et al.*, *Plant Cell* **16**, 1220 (2004).
- W. J. Swanson, V. D. Vacquier, *Nat. Rev. Genet.* **3**, 137 (2002).
- A. Kachroo, M. E. Nasrallah, J. B. Nasrallah, *Plant Cell* **14**, S227 (2002).
- Supported by the University of Zürich, grants from the Swiss National Science Foundation (U.G.) and the National Science Foundation of China (W.-C.Y.), and a Human Frontier Science Program fellowship (S.K.). We thank C. Baroux and P. Barrell for help with confocal analyses; D. Weigel and J.-E. Faure for seeds; M. Curtis, R. Blainvillain, and P. Gallois for plasmids; P. Kopf for technical assistance; and M. A. Collinge and S. E. Schauer for discussions and comments on the manuscript. GenBank accession numbers for FER homologs are as follows: *B. oleracea*, EF681131; *A. lyrata*, EF681133; *A. thaliana* L-er, EF681137; *C. flexuosa* 1, EF681134; *C. flexuosa* 2, EF681135; *C. flexuosa* 3, EF681136; *C. flexuosa* 4, EF681132.

Supporting Online Material

www.sciencemag.org/cgi/content/full/317/5838/656/DC1

Materials and Methods

Fig. S1

Table S1

References

9 April 2007; accepted 14 June 2007

10.1126/science.1143562

Quantitative Mass Spectrometry Identifies Insulin Signaling Targets in *C. elegans*

Meng-Qiu Dong,¹ John D. Venable,¹ Nora Au,^{2,3} Tao Xu,¹ Sung Kyu Park,¹ Daniel Cociorva,¹ Jeffrey R. Johnson,¹ Andrew Dillin,² John R. Yates III^{1*}

DAF-2, an insulin receptor–like protein, regulates metabolism, development, and aging in *Caenorhabditis elegans*. In a quantitative proteomic study, we identified 86 proteins that were more or less abundant in long-lived *daf-2* mutant worms than in wild-type worms. Genetic studies on a subset of these proteins indicated that they act in one or more processes regulated by DAF-2, including entry into the dauer developmental stage and aging. In particular, we discovered a compensatory mechanism activated in response to reduced DAF-2 signaling, which involves the protein phosphatase calcineurin.

The insulin signaling pathway and insulin-like growth factor–1 (IGF-1) signaling pathway are conserved from invertebrates to mammals (1, 2). DAF-2, the sole homolog of the insulin receptor or IGF-1 receptor in *C. elegans*, controls the expression of presumably a large number of downstream targets by negatively

regulating DAF-16, a FoxO transcription factor (3–8). In this study, we integrated technological advancements in quantitative mass spectrometry (MS) (9–11), including labeling multicellular organisms with the ¹⁵N stable isotope, to identify DAF-2 signaling targets. We made direct measurements of proteins as opposed to mRNAs, which are not final gene products. Our method allows for the identification of targets not regulated at the transcription level. The MS techniques demonstrated in this study can be readily used to determine protein abundance changes as a result of genetic or pharmacological perturbations.

We prepared lysates from wild-type (WT), *daf-16(mu86)* null, or *daf-2(e1370ts)* worms in their first day of adulthood, a period important for regulation of longevity by DAF-2 signaling (8). These lysate samples were mixed at a 1:1 ratio with a reference sample in which all proteins were labeled with ¹⁵N (atomic enrichment of ¹⁵N ≥ 96%) [(12) and fig. S1]. This reference sample was a lysate of WT worms fed with bacteria that were grown in a medium enriched in ¹⁵N. Soluble proteins (S100 fraction) from the lysate mixtures were then digested and analyzed by MS. A total of 1685 proteins were identified. Using its ¹⁵N-labeled counterpart as a reference, we determined the relative abundance of each unlabeled (i.e., ¹⁴N-labeled) protein with a modified version of the RelEx software (10). We also assessed the relative abundance of individual proteins by spectral counting (SC), in which we counted how many times the unlabeled version of a protein was identified by the fragmentation spectra of its peptides. Spectral counts correlate with protein abundance (11). We detected little difference between the *daf-16* and WT samples (fig. S2A), reflecting the fact that *daf-16* and WT adult worms were phenotypically similar under our experimental conditions (3, 4, 6–8). In contrast, we observed many protein abundance changes in the *daf-2* mutants as compared with those in WT worms (fig. S2B), with an obvious correlation (i) between the RelEx and SC measurements ($r = 0.59$) and (ii) between the

¹Scripps Research Institute, La Jolla, CA 92037, USA. ²Salk Institute for Biological Studies, La Jolla, CA 92037, USA. ³University of California at San Diego, La Jolla, CA 92093, USA.

*To whom correspondence should be addressed. E-mail: jyates@scripps.edu

ERRATUM

Post date 3 October 2008

Reports: “The FERONIA receptor-like kinase mediates male-female interactions during pollen tube reception” by J.-M. Escobar-Restrepo *et al.* (3 August 2007, p. 656). On page 657, second column, second paragraph, the sentence “The *FER* open reading frame contains a single 175-bp intron in the 5′ untranslated region and produces a transcript of 2682 bp, which encodes a putative receptor-like serine-threonine kinase (RLK) (Fig. 1F)” contains two errors. It should read, “The *FER* primary transcript contains a single 175-bp intron in the 5′ untranslated region and produces an open reading frame of 2682 bp, which encodes a putative receptor-like serine-threonine kinase (RLK) (Fig. 1F).”



The FERONIA Receptor-like Kinase Mediates Male-Female Interactions During Pollen Tube Reception

Juan-Miguel Escobar-Restrepo, Norbert Huck, Sharon Kessler, Valeria Gagliardini, Jacqueline Gheyselinck, Wei-Cai Yang and Ueli Grossniklaus (August 3, 2007)
Science 317 (5838), 656-660. [doi: 10.1126/science.1143562]

Editor's Summary

This copy is for your personal, non-commercial use only.

- Article Tools** Visit the online version of this article to access the personalization and article tools:
<http://science.sciencemag.org/content/317/5838/656>
- Permissions** Obtain information about reproducing this article:
<http://www.sciencemag.org/about/permissions.dtl>

Science (print ISSN 0036-8075; online ISSN 1095-9203) is published weekly, except the last week in December, by the American Association for the Advancement of Science, 1200 New York Avenue NW, Washington, DC 20005. Copyright 2016 by the American Association for the Advancement of Science; all rights reserved. The title *Science* is a registered trademark of AAAS.